Estimation Architectures for Precise Time and Frequency Transfer in a LEO Constellation

Christopher Flood, Penina Axelrad
[1]CCAR and Smead Aerospace Engineering Sciences
University of Colorado Boulder
Boulder, CO, 80303, USA
christopher.flood@colorado.edu

Andrew J. Metcalf
[2]Space Vehicles Directorate
Air Force Research Laboratory
Albuquerque, NM, 87123, USA

Benjamin K. Stuhl[2,3]
[3]Space Dynamics Laboratory
Utah State University
North Logan, UT, 84341, USA

***Summary*— This work explores centralized and decentralized estimation architectures designed for time and frequency transfer via optical inter-satellite links in a LEO constellation.**

Keywords—optical links, synchronization, estimation

I. INTRODUCTION

In recent years, ground-based optical systems have been used for satellite ranging to support orbit determination [1], ground-to-space communication [2], and time transfer [3]. Conventional methods of satellite telemetry, tracking, and control (TTC) require one-to-one contact with specific ground stations, limiting satellite updates to periods when it is in view of a particular ground station. This model has historically worked well, with the onus of TTC spread across a number of independent spacecraft operators, and relatively small satellite constellation sizes (<100). Over the past 5 years this paradigm has changed, as mega-constellations of small satellites (Starlink, Kuiper, OneWeb, Telesat) are currently being populated [4] to support worldwide broadband access, Earth observation, and various commercial and science goals. At the same time, research and development of space-qualified optical hardware has resulted in the deployment of large optical communication terminals [5] serving as the backbone of ESA's space data highway and other high data rate applications. Miniature versions of these optical terminals [6] have the capability to enable communication, ranging, and time transfer between small satellites in a constellation. The exponential growth in constellation size and the increase in technology readiness level of optical terminals present an opportunity for analysis of the impact of inter-satellite links on increased constellation autonomy.

We present the analysis of potential time and frequency transfer methods among satellites in a low Earth orbit (LEO) constellation, based on optical inter-satellite links (OISL) typically used for communication. Our simulation considers an expanded functionality of the optical terminals to support dual one-way time transfer, with the goal of achieving clock synchronization across the constellation at the 5-100ps level. The capability for synchronization over an optical communications channel at this level was demonstrated for ground-based links [7]. This work addresses three elements – 1) modeling inter-satellite ranging measurements with realistic accuracy based on results reported in [3,8]; 2) characterizing the impact of measurement intervals on the clock estimation; and 3) estimation methods to achieve high precision time and frequency (T&F) transfer across the constellation in a computationally efficient manner.

Approved for public release; distribution is unlimited. Public Affairs release approval AFRL- 2022-2405. This work was supported by AFRL grant FA9453-19-1-0076 to the University of Colorado Boulder. The views expressed are those of the authors and do not reflect the official guidance or position of the United States Government, the Department of Defense, or of the United States Air Force.

II. METHODS

A. Satellite Constellation

A Walker Star [9] constellation with parameters 89°:180/18/2 is similar to proposed LEO constellations. This constellation is designed using NASA's open source mission design software [10], the General Mission Analysis Tool (GMAT). GMAT enables the use of high-fidelity orbit dynamics, such as Earth's gravity field and point mass influence from third bodies, as well as suite of propagation methods to choose from. GMAT can be used through the graphical user interface (GUI) or the application programming interface (API) for integration into languages such as MATLAB, Python, or Java - this project uses the GMAT API in MATLAB.

B. Clock Model

Clocks on each satellite in the constellation are modeled by creating a clock offset and frequency profile for the duration of the simulation. The clock signatures are generated using a discrete time, two-state clock model as derived in [11-12], and additionally shown (1 – 4) below.

$$x(t_{k+1}) = \Phi(\Delta t)x(t_k) + w(t_k) \tag{1}$$

$$\Phi(\Delta t) = \begin{bmatrix} 1 & \Delta t \\ 0 & 1 \end{bmatrix} \tag{2}$$

$$w(t_k) \sim N(0, Q) \tag{3}$$

$$Q(\Delta t) = \begin{pmatrix} q_1 \Delta t + \frac{q_2 \Delta t^3}{3} & \frac{q_2 \Delta t^2}{2} \\ \frac{q_2 \Delta t^2}{2} & q_2 \Delta t \end{pmatrix} \tag{4}$$

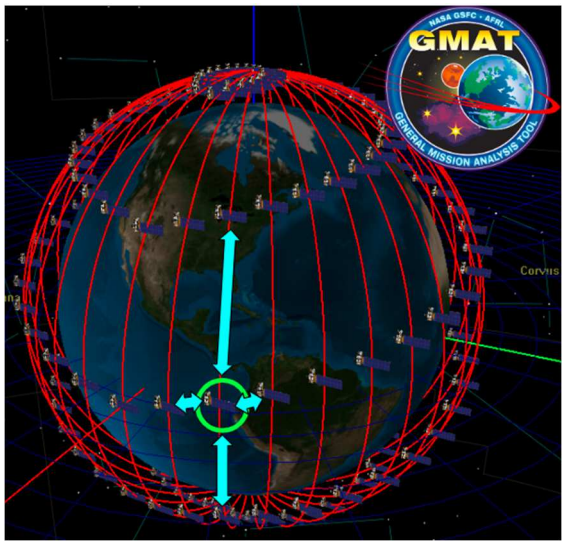

Fig. 1. Simulated Walker Star satellite constellation with inter-satellite links (blue arrows) shown for a single satellite (circled)

The values for q in (4) are determined by the Allan deviation (ADEV) specification of the clock that is being numerically simulated [11]. The clocks are simulated to represent Excelitas rubidium atomic frequency standards (RAFS) , which have years of spaceflight heritage on the Global Positioning System (GPS) satellites [13]. Recent trends in atomic clock development [14] suggest that a low-SWaP atomic clock with RAFS-like performance could fly on a small satellite in the next few years.

C. Measurement Model

Optical communication terminals are assumed to be located on the radial, ± in-track, and ± cross-track body axes of the spacecraft to simulate links between members of the constellation. The OISL could be used for communication in addition to ranging measurements for time transfer. A set of measurements is generated between satellites which satisfy the following criteria: 1) no Earth obstruction and 2) line-of-sight vector is within 20° of the boresight for both the transmitting and receiving OISL terminals. The inter-satellite links are restricted to in-plane and adjacent plane connections to limit the number of connections in large satellite constellations, without inhibiting the flow of information.

The range measurements are created by computing the signal time-of-flight between the transmitter and receiver, accounting for the additional travel time due to the receiver platform motion. The coordinate time of signal reception is T_{rx} and the coordinate time of signal transmission is T_{tx}. The effect of transmitter and receiver clock errors is included on the range measurement, represented by $b_B(T_{rx})$ as the clock offset of the receiver at the time of signal reception and $b_A(T_{tx})$ as the clock offset of the transmitter at the time of signal transmission. The inter-satellite range measurement model is shown in (5).

$$\rho_{AB} = c\cdot[T_{rx} - T_{tx} + b_B(T_{rx}) - b_A(T_{tx})] + \sigma_{noise} \qquad (5)$$

The magnitude of the measurement noise in (5) has a significant impact on the ability to estimate the clock states and transfer time. A small measurement noise will result in a better clock estimate, but may not be a realistic representation of noise figures in existing optical systems. Current literature [8] suggests that the range for this noise figure is 30 – 100ps. The lower boundary is from the Atomic Clock Ensemble in Space (ACES) optical time transfer system [15] and the upper boundary is based on reported values of the Time Transfer by Laser Link (T2L2) system [16]. This information is used to establish realistic bounds on the levels of measurement noise that we should consider.

The interval between consecutive measurements affects the quality of the clock estimate. Due to frequency errors in the simulated clocks, the clocks will deviate from the reference time between measurements. If the measurement interval is small and the oscillators are sufficiently stable, it is possible to estimate the clocks with errors below the measurement noise as the measurement noise can be averaged out over time. However, other aspects of the satellite constellation, such as communication and processing latency, may impose a lower limit on the measurement interval size. Different measurement intervals of 1, 10, and 60 seconds are used to characterized the effect of the measurement interval on the clock estimation.

D. Estimation

The truth position and velocity ephemerides were generated by propagating each satellite state with GMAT at a 1 second time step. The clock signatures were created in parallel using a two-state clock model and process noise generated from the noise statistics of the RAFS clock. Inter-satellite range measurements were also generated at 1 second measurement intervals between valid satellite combinations. The measurements are processed in a conventional Kalman Filter (CKF) to estimate the offset and frequency of the clocks in the satellite constellation.

The standard application of a CKF to this problem is to have one state estimate of all the clocks, a single state prediction step, and a single measurement update which uses all the measurements at once. This is easy to do in simulation and yields good estimation results, but implies the following: 1) transmission of all measurements to a central location, 2) the back propagation of the measurement updated state to each member of the constellation, and 3) a processing latency of the filter that is faster than the measurement rate. As constellations grow with size, this centralized approach does not scale well.

An alternative is a decentralized estimation approach which fuses data using covariance intersection methods [17]. In this architecture each member of the constellation maintains a local copy of the entire constellation state and the time update remains the same as in the centralized case. The local measurement update consists of three steps: 1) perform the measurement update with range measurements made locally, 2) broadcast your measurement updated state to all directly linked satellites, 3) fuse your pre-measurement updated covariance (6) and state (7) with the post-measurement updated covariance and states received from neighboring satellites, and 4) use the measurements made locally for a final measurement update

with the fused state estimate. This process ensures that information is not reused and that correlations between state estimates in the constellation are correctly captured.

Equation (6) shows the process for fusing 2 covariance matrices by adding the information matrices ($\mathbf{P}^{-1}_{xx}$) scaled by individual weights (ω). Once the fused covariance is computed, (7) can be used to solve for the fused state variable, $\mathbf{c}$. We extend these equations to N estimates and use equal weights for the clock state fusion.

$$\mathbf{P}^{-1}_{cc} = \omega\, \mathbf{P}^{-1}_{aa} + (1 - \omega)\, \mathbf{P}^{-1}_{bb} \tag{6}$$

$$\mathbf{P}^{-1}_{cc}\mathbf{c} = \omega\, \mathbf{P}^{-1}_{aa}\mathbf{a} + (1 - \omega)\, \mathbf{P}^{-1}_{bb}\mathbf{b} \tag{7}$$

The same reference ephemerides, measurements, and initial state offset are used in both the centralized and decentralized estimation architectures to enable comparison between the two methods.

III. RESULTS

We consider 12 unique scenarios with the possible measurement rates (1, 10, and 60 seconds), measurement noise values (30 and 100 picoseconds), and estimation methods (centralized and decentralized). 10 realizations were run for a subset of the scenarios to ensure results did not occur by chance. Examples of the clock offset error results are shown in Fig. 2 and Fig. 3 for a single satellite.

A. Centralized Estimation

Fig. 2 shows the clock offset error for a single satellite with a centralized estimation architecture with different measurement rates and measurement noise values. As the measurement noise and time between measurements increases, the clock offset error and uncertainty grow larger. The change from Fig. 2a to Fig. 2b is small due to the short measurement interval of 1 second. In Fig. 2c and Fig 2d the clock offset uncertainty grows between measurements and creates a "saw tooth" pattern. The effect of the increase in measurement noise from Fig. 2c to Fig. 2d is more pronounced as a result of the longer measurement interval of one observation per minute.

B. Decentralized Estimation

In the decentralized estimation architecture each satellite has an estimated clock state history for the entire constellation; however, only the measurements made by the satellite are used directly and all other clock information converges through fusion of the shared estimates. Fig. 3 shows the clock offset error for the same satellite in Fig. 2, but using decentralized estimation methods. As the measurement noise and time between measurements increase, the clock estimation quality decreases.

C. Method Comparison

Fig. 2 and Fig. 3 show the clock offset error for the same satellite, measurement noise values, and measurement rates with the only difference being the estimation method used. The degradation of the clock estimation as a function of the estimation method can be seen by comparing Fig. 2 and Fig. 3. In each scenario shown, the decentralized approach yields worse results than the centralized approach. This follows intuition as the decentralized method is using fewer range measurements, and thus less information, than the centralized method. However, the decentralized method is only worse by a factor of 2-4. If the benefits of using a decentralized approach outweigh the degradation in estimation quality, that expands the number of options for the mission designer.

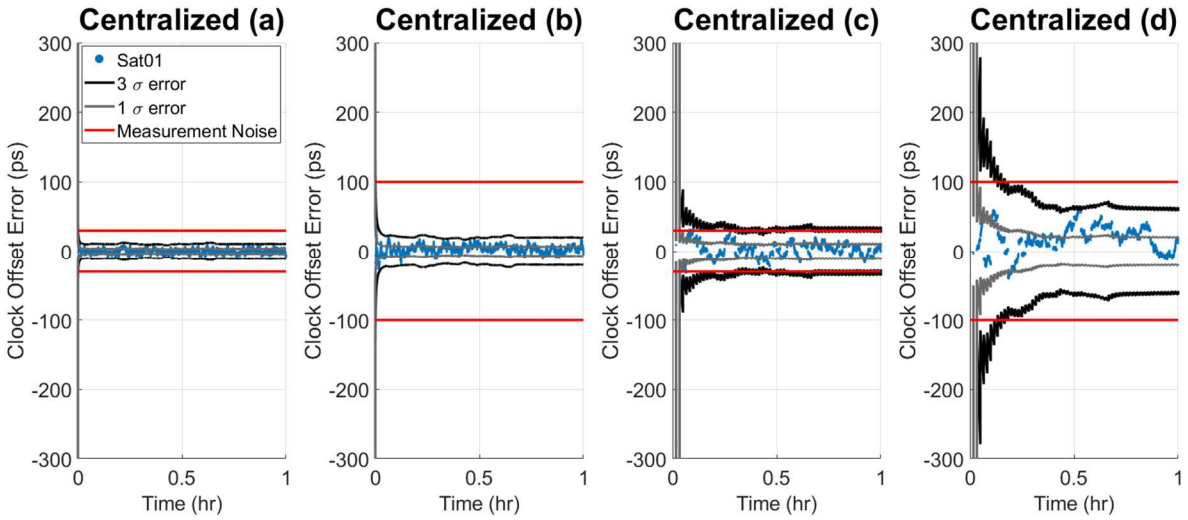

Fig. 2. Time transfer error for a single satellite using a centralized estimation architecture. From left to right: a) 1s measurement rate, 30ps noise b) 1s measurement rate, 100ps noise, c) 60s measurement rate, 30ps noise, d) 60s measurement rate, 100ps noise

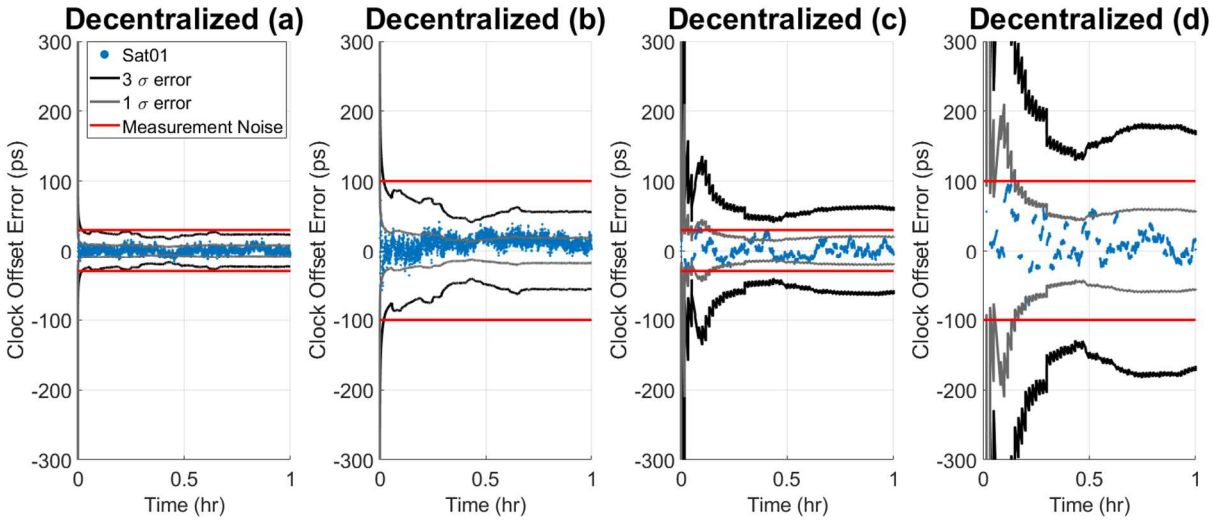

Fig. 3. Time transfer error for a single satellite using a decentralized estimation architecture. From left to right: a) 1s measurement rate, 30ps noise b) 1s measurement rate, 100ps noise, c) 60s measurement rate, 30ps noise, d) 60s measurement rate, 100ps noise

The estimation methods are compared at the constellation level by aggregating the clock offset errors of the all satellites and treating them as a random variable. Different time thresholds are selected and the percent of the error within these thresholds is used as a single metric to represent the estimation quality. The results are shown in Table 1 and Table 2 for time thresholds of 5, 10, 50, and 100 picoseconds.

TABLE I. CENTRALIZED ESTIMATION RESULTS

Interval	Noise	5ps	10ps	50ps	100ps
1s	30ps	82%	99%	100%	100%
1s	100ps	52%	84%	>99%	>99%
10s	30ps	53%	85%	>99%	>99%
10s	100ps	29%	53%	99%	>99%
60s	30ps	33%	60%	98%	98%
60s	100ps	16%	30%	91%	98%

TABLE II. DECENTRALIZED ESTIMATION RESULTS

Interval	Noise	5ps	10ps	50ps	100ps
1s	30ps	67%	95%	>99%	>99%
1s	100ps	35%	63%	>99%	>99%
10s	30ps	45%	76%	>99%	>99%
10s	100ps	22%	41%	97%	>99%
60s	30ps	28%	51%	97%	98%
60s	100ps	12%	22%	78%	91%

IV. DISCUSSION

The results in the tables above show that there are a variety of configurations that enable constellation synchronization for different time thresholds. A time threshold can be selected based on the application and then the optimal arrangement that supports that timing threshold can be chosen based on the needs of the constellation designer. For a 100 picosecond timing threshold, there are 11 different options to choose from in order to meet that timing requirement for >98% of the time. This enables mission designers to make trades between the measurement rate, the measurement noise of the on-board equipment, and the data processing requirements. A stricter timing requirement of 10 picoseconds results in fewer viable options - the only option that satisfies this timing threshold is the shortest measurement interval, the smallest measurement noise, and the centralized estimation architecture.

V. CONCLUSIONS

This work describes scalable clock estimation architectures that support time and frequency transfer between small satellites in a constellation. Centralized estimation methods provide the smallest clock offset error, but impose potentially significant communication requirements that scale poorly with increasing constellation size. The decentralized estimation method results in increased clock errors, but is a more practical method to implement that scales better with a growing number of participants. It was shown that for 50 and 100 picosecond timing requirements there exist an assortment of options that achieve those levels of synchronization.

Future work includes increasing the fidelity of the measurement and dynamic model, including the effect of trajectory errors and relativistic corrections. Trajectory errors can by generated through the addition of random noise or in a more structured manner such as using Hill's equations or a slightly perturbed dynamic model in the CKF. Errors in the satellite ephemerides can impact the ability to transfer time / frequency [18] as well as the computation of relativistic frequency corrections [19].

Additional stability analysis will be conducted of the theoretical timescale produced by ensembling all clocks in the constellation. The number of participants in the proposed constellations provides an opportunity for a large clock ensemble, which is capable of producing a timescale with stability that increases with the constellation size and additional resilience in the case of single or multiple clock failures.

REFERENCES

[1] B.D. Tapley, B.E. Schutz, and, R.J. Eanes (1985) “Satellite laser ranging and its applications,” Celestial Mechanics vol. 37, pp. 247–261.

[2] D. M. Boroson, et al. (2014) "Overview and results of the lunar laser communication demonstration," Proc. SPIE 8971, Free-Space Laser Communication and Atmospheric Propagation XXVI, 89710S.

[3] P. Guillemot, P. Exertier, E. Samain, F. Pierron, J.M. Torre, and S. Leon (2009) “Time transfer by laser link - T2L2: results of the first year of operation,” 41st Annual Precise Time and Time Interval (PTTI) Systems and Applications Meeting.

[4] J. C. McDowell (2020) "The low Earth orbit satellite population and impacts of the SpaceX starlink constellation," The Astrophysical Journal vol. 892, L36.

[5] Frank Heine, et al. (2020) "Status of Tesat laser communication activities," Proc. SPIE 11272, Free-Space Laser Communications XXXII, 1127204.

[6] R. W. Kingsbury, J. C. Twichell, and S. E. Palo (2022) "Cobalt optical crosslink terminal," Proc. SPIE 11993, Free-Space Laser Communications XXXIV, 119930N.

[7] I. Khader, et al. (2018) “Time synchronization over a free-space optical communication channel,” Optica, Vol. 5, No.12, pp. 1542-1548.

[8] P. Exertier, et al.(2019) “Time and laser ranging: a window of opportunity for geodesy, navigation, and metrology,” J Geod 93, 2389–2404.

[9] J. G. Walker (1984) “Satellite constellations,” Journal of the British Interplanetary Society, vol. 37, pp. 559-571.

[10] S. P. Hughes (2016) *General Mission Analysis Tool (GMAT)* [Powerpoint Presentation], International Conference of Astrodynamics Tools and Techniques.

[11] L. Galleani (2008) “A tutorial on the two-state model of the atomic clock noise,” Metrologia vol. 45, pp. 175-182.

[12] T. D. Schmidt, C. Trainotti, and J. Furthner (2019) "Comparing clock steering technique performances in simulations and measurements," Proceedings of the 50th Annual Precise Time and Time Interval Systems and Applications Meeting, Reston, Virginia, pp. 290-298.

[13] B. Jaduszliwer, and J. Camparo (2021) “Past, present and future of atomic clocks for GNSS,” GPS Solutions vol. 25.

[14] D. Scherer (2022) “The future of industrial atomic clocks,” Proceedings of the 53rd Annual Precise Time and Time Interval Systems and Applications Meeting, Long Beach, California.

[15] K. U. Schreiber, and J. Kodet (2018) “The application of coherent local time for optical time transfer and the quantification of systematic errors in satellite laser ranging” Space Sci Rev 214, 22.

[16] E.Samain, et al. (2015) “Time transfer by laser link: a complete analysis of the uncertainty budget,” Metrologia. 52.

[17] S. Julier and J. Uhlmann, (2001) “General decentralized data fusion with covariance intersection (CI),” Ch. 12.

[18] L. Duchayne, F. Mercier, and P. Wolf (2009) “Orbit determination for next generation space clocks,” A&A 504 (2) 653-661.

[19] B. Kroese, G. Giorgi and C. Günther (2018) "Relativistic corrections for intersatellite frequency transfer," 2018 European Frequency and Time Forum (EFTF), pp. 240-244.